AD-A042 488 CASE WESTERN RESERVE UNIV CLEVELAND OHIO ELECTROCHEMI--ETC F/G 7/4
AN OVERVIEW OF THE ELECTROCHEMICAL INTERFACE AND OPTICAL SPECTR--ETC(U)
JUN 77 E YEAGER N00014-75-C-0953

UNCLASSIFIED TR-47 NL

| OF |
AD
A042488

END
DATE FILMED
8-77
DDC

AD A042488

(12) 9

ELECTROCHEMISTRY RESEARCH LABORATORIES

DEPARTMENT OF CHEMISTRY

JOHN SCHOFF MILLIS SCIENCE CENTER

CASE WESTERN RESERVE UNIVERSITY

CLEVELAND, OHIO 44106

DDC
AUG 5 1977
C

TECHNICAL REPORT NO. 47

AN OVERVIEW OF THE ELECTROCHEMICAL INTERFACE AND OPTICAL SPECTROSCOPIC STUDIES

by

Ernest Yeager

DISTRIBUTION STATEMENT A
Approved for public release;
Distribution Unlimited

1 June 1977

OFFICE OF NAVAL RESEARCH

Contract N00014-75-C-0953

Project NR 359-451

AD No.____
DDC FILE COPY

OFFICE OF NAVAL RESEARCH

Contract N00014-75-C-0953

Project NR 359-451

TECHNICAL REPORT NO. 47

AN OVERVIEW OF THE ELECTROCHEMICAL INTERFACE AND OPTICAL SPECTROSCOPIC STUDIES

by

Ernest Yeager

Prepared for presentation at the International Colloquium on Optical Properties of Solid-Liquid Interfaces, sponsored by the CNRS in La Colle sur Loup (France) on 23-28 May 1977

Electrochemistry Research Laboratory
Department of Chemistry
CASE WESTERN RESERVE UNIVERSITY
Cleveland, Ohio 44106

1 June 1977

Reproduction in whole or in part is permitted for any purpose of the United States Government

This document has been approved for public release and sale; its distribution is unlimited.

ACCESSION for
NTIS White Section
DDC Buff Section
UNANNOUNCED
JUSTIFICATION
BY
DISTRIBUTION/AVAILABILITY CODES
Dist. SPECIAL
A

SECURITY CLASSIFICATION OF THIS PAGE (When Data Entered)

REPORT DOCUMENTATION PAGE

READ INSTRUCTIONS BEFORE COMPLETING FORM

1. REPORT NUMBER (14) TR-47	2. GOVT ACCESSION NO.
3. RECIPIENT'S CATALOG NUMBER (9)	
4. TITLE (and Subtitle) (6) An Overview of the Electrochemical Interface and Optical Spectroscopic Studies	5. TYPE OF REPORT & PERIOD COVERED Technical Report, #47
	6. PERFORMING ORG. REPORT NUMBER
7. AUTHOR(s) (10) Ernest Yeager	8. CONTRACT OR GRANT NUMBER(s) (15) N00014-75-C-0953
9. PERFORMING ORGANIZATION NAME AND ADDRESS Department of Chemistry Case Western Reserve University Cleveland, Ohio 44106	10. PROGRAM ELEMENT, PROJECT, TASK AREA & WORK UNIT NUMBERS NR-359-451
11. CONTROLLING OFFICE NAME AND ADDRESS Office of Naval Research Chemistry Program - Chemistry Code 472 Arlington, Virginia 22217	12. REPORT DATE (11) 1 June 1977
	13. NUMBER OF PAGES 51
14. MONITORING AGENCY NAME & ADDRESS (if different from Controlling Office) (12) 55p.	15. SECURITY CLASS. (of this report) Unclassified
	15a. DECLASSIFICATION/DOWNGRADING SCHEDULE

16. DISTRIBUTION STATEMENT (of this Report)

Approved for public release; distribution unlimited

17. DISTRIBUTION STATEMENT (of the abstract entered in Block 20, if different from Report)

18. SUPPLEMENTARY NOTES

19. KEY WORDS (Continue on reverse side if necessary and identify by block number)

electrochemical interfaces, ionic double layer, electrosorption

20. ABSTRACT (Continue on reverse side if necessary and identify by block number)

This paper reviews the present understanding of the structure of electrochemical interfaces and identifies the types of information which optical spectroscopic measurements may be able to contribute. Particularly challenging problems are the structure of the solvent in the compact layer and the nature of the interactions of adsorbed species with the electrode surface. So far, little information has been derived from optical measurements concerning these problems.

DD FORM 1 JAN 73 1473 EDITION OF 1 NOV 65 IS OBSOLETE S/N 0102-014-6601 |

Unclassified
SECURITY CLASSIFICATION OF THIS PAGE (When Data Entered)

403 880

15

TABLE OF CONTENTS

LIST OF FIGURES

AN OVERVIEW OF THE ELECTROCHEMICAL INTERFACE AND OPTICAL SPECTROSCOPIC STUDIES

Ernest Yeager
Case Laboratories for Electrochemical Studies
and The Chemistry Department
Case Western Reserve University
Cleveland, Ohio 44106, USA

I. INTRODUCTION

The purpose of this lecture is two-fold: 1) to review the present understanding of the structure of electrochemical interfaces; and 2) to identify the types of information which optical measurements may be able to contribute.

The structure of the electrochemical interface is a particularly challenging problem. A quantitative description is essential to the orderly development of electrochemical surface science and yet even the qualitative description of the interface remains in doubt, despite a very substantial literature on this topic (for review see ref. 1-3). Electrochemical interfaces usually involve steep potential gradients and strong interactions of the solvent and other electrolyte phase species with the metal or semiconductor electrode surface as well as with other electrolyte phase components. This means that discrete charge effects and discrete interactions must be taken into account in any reliable theoretical model. On the other hand, very little information is available concerning the chemical interactions of the adsorbed species with the electrode and the adsorption sites. The extrapolation of solid-gas information concerning interaction energies, configurations and adsorption sites to electrochemical interfaces is precarious since the interactions of the various adsorbed species with the electrolyte phase components (particularly the solvent) are usually strong.

Part of the problem is a general lack of good molecularly specific experimental techniques for examining the chemical structures of electrochemical interfaces, analogous to the various spectroscopic techniques which have proved so helpful in establishing the molecular structure and interaction chemistry in the bulk gas and condensed phases. In many instances electrochemical measurements provide sensitive tools for the detection of changes in the structure of the electrochemical interface and particularly the adsorption of various species even down to small fractions of a monoloayer, but they lack the needed molecular level specificity to identify the nature of the surface interactions. Even the charge on electrosorbed species cannot be determined electrochemically because of the difficulty of resolving what fraction of the externally provided charge is transferred to the adsorbed species rather than just residing on the metal surface, compensating the charge of the electrosorbed species and the remainder of the ionic double layer (see, e.g., ref. 4-8).

The most promising general experimental approach for obtaining molecular level information is <u>in situ</u> optical spectroscopy. Tables 1 and 2 summarize the various optical spectroscopic techniques which are available for <u>in situ</u> studies of electrochemical interfaces and the types of information which the electrochemist may hope to derive from such measurements. The literature contains reports of the use of all of these methods with some degree of success in electrochemical studies, with the exception of photo-acoustic spectroscopy.[+] Ultraviolet-visible reflectance spectroscopy

---

[+] Photo-acoustic spectroscopy involves the determination of the optical absorption spectrum of surface layers by illiminating the surface with modulated monochromatic light and then detecting the optical absorption through the thermally generated sound in the ambient phase as a function of optical wavelength. This method lends itself to surfaces of very poor optical quality such as high area catalyst layers and should prove useful for examining the valency state of various electrocatalysts.

including ellipsometric spectroscopy are sensitive to the surface electronic properties of metal and semiconductors and changes in these properties produced by interactions with various species originating from the electrolyte phase. Ultraviolet-visible spectroscopy can also provide chemical information concerning catalyst layers, passivation layers and in general the various mono- and multi-layers which play a critical role in controlling electrochemical processes. A number of electrochemists have made use of these optical techniques to study electrochemical interfaces and particularly electrosorption and passivation over the past decade. To date these studies have contributed relatively little further understanding concerning the electronic-chemical features of the interface. Substantial information is contained in the UV-visible reflectance and ellipsometric data; the problem is to extract and interpret this information. This problem is not restricted to electrochemical interfaces.

Vibrational data for adsorbed species including water itself would be quite helpful. In situ infrared studies have been carried out (10,11) using multiple attenuated total reflection techniques and infrared transparent electrode substrates, but have not yielded much information concerning adsorbed species. Solvent absorption and sensitivity have been serious problems. In situ Raman (13a,b,c), including resonant Raman (14,15) where applicable, may prove more promising for studies of adsorbed species, particularly since water is not a problem.

It is unfortunate that the elegant surface physics techniques such as LEED, UPS, XPS and Auger cannot be applied in situ to electrochemical studies. Even so, efforts are in progress to use these techniques ex situ in electrochemical studies with special procedures for minimizing structural changes during the transfer between the electrochemical and high vacuum

environments (16-21). Despite the special features of electrochemical interfaces, parallel solid-gas and electrode-electrolyte interface studies should prove quite helpful in better understanding electrochemical interfaces.

II. Basic Structural Features of Electrochemical Interfaces

A. The Diffuse Layer

The ionic double layer on the electrolyte side of the electrochemical interface is considered to consist of two regions: a Helmholtz or compact layer across which most of the potential drop occurs, and a diffuse ionic layer (Gouy-Chapman) extending out into the electrolyte phase (see Fig. 1a). The diffuse ionic layer presents no problem for solutions sufficiently dilute that point charge treatments in a dielectric continuum are applicable (see ref. 1-3, 42). For a symmetrical electrolyte ($z_+ = z_- = z$), the potential distribution is given by

$$\phi = \frac{4kT}{ze} \tanh^{-1} \exp[p - \kappa x] \tag{1}$$

where the Debye reciprocal length κ is given by

$$\kappa^2 = \frac{8\pi z^2 e^2}{\varepsilon kT} c \tag{1a}$$

and

$$p = \ln \tanh[\frac{ze\phi_2}{4kT}] + \kappa x_2 \tag{1b}$$

ε is the dielectric constant of the solvent, c is the bulk concentration of the electrolyte and the subscript 2 corresponds to the plane of closest approach of the solvated ions to the electrode surface, i.e. the outer Helmholtz plane (see Fig. 2). For large values of $x - x_2$, the potential dependence approaches the form

$$\phi = A \exp -\kappa x \tag{2}$$

In electrochemical reactions, the position x_2 is often considered as the pre-reaction state for non-specifically adosrbed species prior to the charge transfer process. The concentration of charged reacting species in this plane can be calculated from ϕ_2. Further the potential drop across the Helmholtz layer ($\phi_m - \phi_2$) controls the height of the potential energy barrier for the charge transfer process. Consequently ϕ_2 is needed in order to correct for ionic double layer effects in electrode kinetic studies. This potential can be calculated from the net charge, q, in the ionic double layer in the absence of specific ionic adsorption using the equation

$$q = (q_+)_{2-s} + (q_-)_{2-s} \tag{3}$$

where $$(q_+)_{2-s} = \left(\frac{RT\varepsilon}{2\pi}\, c\right)^{1/2}\left[\exp - \frac{z_+\varepsilon\phi_2}{2kT} - 1\right] \tag{3a}$$

and $$(q_-)_{2-s} = -\left(\frac{RT\varepsilon}{2\pi}\, c\right)^{1/2}\left[\exp - \frac{z_-\varepsilon\phi_2}{2kT} - 1\right] \tag{3b}$$

The charge q can be determined from experimental data for the differential capacitance C using the equation

$$q = \int_{E_{pzc}}^{E} C\, dE \tag{4}$$

where E is the electrode potential relative to a reference electrode and E_{pzc} is the corresponding value when q = 0, i.e. the potential of zero charge (pzc). At the pzc, the potential drop across the interface should be only that associated with the surface dipoles and hence close to zero. Alternatively, with liquid metal electrodes the charge q can also be evaluated from the interfacial tension γ using the Lippmann equation (27)

$$q = -(\partial\gamma/\partial E)_{\mu_i} \qquad (5)$$

with the chemical potentials of all bulk components kept constant.

The Gouy-Chapman treatment is a dilute solution theory and breaks down at practical concentrations ($\geq$ 0.1 M). Factors which contribute to this breakdown include the non-ideality of the solvent as a dielectric, the polarizability of the ions and short range repulsion effects. Various workers have attempted to extend the Gouy-Chapman treatment by taking into account dielectric saturation (25, 26) and the dependence of the dielectric constant on electrolyte concentration. Several theorists have used statistical mechanical methods to develop treatments applicable to higher concentrations (see eq. 3, 28-30). Barlow (3) has treated the diffuse layer using cluster theory in a manner analogous to Friedman's treatment of electrolytes (23).

At concentrations of $\sim$ 1 M and higher, the Debye length ($1/\kappa$) approaches the dimensions of the solvated ions and the Gouy-Chapman layer is no longer really diffuse. All of the presently available treatments become questionable. Fortunately in concentrated electrolytes, the fraction of the potential drop across this layer becomes a small fraction of the total drop across the interface, and hence the potential drop across the "diffuse" layer no longer has much effect on specific ionic adsorption, the kinetics of electrode reactions or the capacitance of the interface.

B. The Compact Double Layer

Much attention has been focused by electrochemists on the compact double layer because of its imporance to the understanding of electrochemical kinetics. The most widely accepted model is that shown in Fig. 2 as proposed by Bockris, Devanathan and Müller (22) for a negatively charged

electrode in an electrolyte such as NaCl. The cations usually interact much more strongly with the solvent in the inner coordination sphere than do the anions. Consequently the cations are shown to approach in significant numbers onto an outer Helmholtz plane position (x_2 in Fig. 1b) with essentially two water molecules interposed between them and the electrode. The barriers for anion adsorption with the exception of fluoride anions are much lower and hence they are able relatively easily to approach directly to the electrode surface. Thus "specific" adsorption occurs with the orbitals of the anions interacting directly with orbitals of the metal. If the chemical interaction is sufficiently strong, the anions will be specifically adsorbed even if the metal is negatively charged, as in Fig. 2. A similar situation can occur for cations but the interaction with the electrode must be usually stronger than with most anions in order to offset the larger solvation energy. Figure 3 indicates the potential energy-distance relation corresponding to cations and anions in Fig. 2. The potential of zero charge is shifted by specific ionic adsorption [the Esin-Markov effect (30)].

Various chemical physicists and electrochemists have attempted to develop a theoretical description of the compact double layer both with and without specific ionic adsorption. The test for these treatments has generally been their ability to account for the differential capacitance of the Hg interface as functions of charge or potential and electrolyte concentration. The diffuse and compact double layer contributions to the overall differential capacitance of the interface are generally represented by two capacitances in series. Thus

$$\frac{1}{C} = \frac{1}{C_{m-2}} + \frac{1}{C_{2-s}} \qquad (6)$$

The diffuse layer component C_{m-2} can be evaluated from eqs. 3, 3a, 3b and for a symmetrical electrolyte is

$$C_{2-s} = \left(\frac{z^2e^2\varepsilon c}{2\pi kT}\right)^{\frac{1}{2}} \cosh\left(\frac{ze\phi_2}{2kT}\right) \qquad (7)$$

This equation indicates that the diffuse layer contribution goes through a minimum at $\phi_2 = 0$ and hence at $E = E_{pzc}$. Further, C_{2-s} is very large compared to the experimentally observed C except in dilute solutions and even then except at potentials close to E_{pzc}. This then facilitates the evaluation of the compact layer capacitance C_{m-2} since in solutions of $\geq$ 0.1 M, $C_{m-2} \cong C$ to a good approximation even at E_{pzc} and furthermore in dilute solutions it is possible to calculate C_{2-s} reasonably reliably (see Fig. 4).

In general the comparison of theory and experiment in terms of C_{m-2} and its potential dependence has not been impressive. The hump in the curve at potentials positive to E_{pzc} (Fig. 4) has been a rather critical test of the various models, one that most treatments have not satisfactorially met. Special note is taken of the intriguing treatment of Buff and Slillinger (30) who use the cluster methods of statistical mechanics. Unfortunately they assume that the interactions introduce only a small perturbation in the behavior of particles whose motion is otherwise uncoupled, independent and random.

Many treatments of the compact double layer involve two-state models for water (e.g. 22, 24, 26, 34-36) where the two states may correspond to orientation of the water dipole toward or away from the surface as shown in Fig. 2. Recently Damaskin and Frumkin (37) have proposed a model (without specific ionic adsorption) in which the water at the interface of the Hg electrode exists in small clusters with chemisorption of individual water molecules occurring at more positive electrode potentials. The

clusters are assumed to have a small dipole moment which can be oriented either toward or away from the surface. Parsons (39) and Damashen (38) have refined the treatment of this model and obtain reasonably good fits to the experimental capacitance vs. charge data, even considering the several somewhat adjustable parameters. Damaskin used Boltzmann statistics to calculate the surface concentration of the cluster, assuming that the clusters consist of a fixed number of water molecules (n) and have their dipole moments oriented toward ($N\uparrow_c$) or away ($N\downarrow_c$) from the electrode surface. Thus if N_T is the total number of entities on the surface, then

$$N_T = N\uparrow_c + N\downarrow_c + N_{ad} \tag{8}$$

where

$$N\uparrow_c/N_T = (1/f_o) \exp (\mu_c X/kT) \tag{8a}$$

$$N\downarrow_c/N_T = (1/f_o) \exp (-\mu_c X/kT) \tag{8b}$$

$$N_{ad}/N_T = (1/f_o) \exp [(-U + \mu_{ad} X)/kT] \tag{8c}$$

with the function f_o

$$f_o = \exp(\mu_c X/kT) + \exp(-\mu_c X/kT) + \exp[(-U + \mu_{ad} X)/kT] \tag{8d}$$

and N_{ad} corresponds to the chemisorbed water molecules with the dipole moment μ_{ad} and specific adsorption energy U at zero field X. Damaskin assigns an area to each of these three species and imposes a conservation of surface area condition. The potential drop across the compact layer $\phi = \phi_m - \phi_2$ is then assumed to be

$$\Delta\phi = \Delta\psi + \Delta\chi \tag{9}$$

where the outer potential contribution $\Delta\psi$ is given by

$$\Delta\psi = \frac{4\pi x_2}{\varepsilon} q \tag{9a}$$

and the surface potential contribution is

$$\Delta\chi = \frac{-4\pi}{\varepsilon} \Sigma N_i \mu_i \tag{9b}$$

and i corresponds to the two orientations of the water clusters and the chemisorbed water; q is the electrode charge. Damaskin takes into account the discreteness of the charge by introduction of a coefficient λ which is intended to take into account the action of the field of all other dipoles on the particular dipole under consideration. Thus

$$X = \frac{4\pi q}{\varepsilon} + \lambda \frac{\Delta\chi}{x_2} = \frac{\Delta\phi}{x_2} \tag{10}$$

Differentiation of $\Delta\phi$ with respect to charge then leads to an expression for the capacitance contribution of the compact double layer as a function of several parameters including the dipole moments of the water clusters and chemisorbed waters, the thickness x_2, the discreteness factor λ and the number of water molecules per cluster. Figure 5 compares the theoretical and experimental values of C vs q with a reasonable choice of these parameters and their temperature dependence and with λ taken as unity. Damaskin concludes from such comparisons that the number of water molecules per cluster is $\sim$3 at 0°C and $\sim$2 at 85°C and also that the dipole moment of the chemisorbed water is much larger (μ_{ad}=3.68D) than the usual value (μ_{H_2O}=1.84D). The increment in the compact layer separations at more positive charge density is caused by water chemisorption according to this model. The temperature dependence shown in Fig. 6 duplicates the major features of the C vs. q experimental data, including the temperature invariant point at 5μC/cm^2.

Similar theoretical results have been obtained by Parsons (39), who has extended the Damaskin-Frumkin model to four states: individual solvent molecules with their dipole moments perpendicular to the surface and toward or away from the metal; and clusters also with their net dipole moments toward or away from the metal. Parsons concludes that the most probable size of the clusters ar room temperature is 3 or 4 with the total dipole of the cluster equal to approximately that for a single molecule. Parsons points out that small ring clusters of water molecules have some stability on the basis of the theoretical considerations of Del Bene and Pople (41). On the basis of the three-water molecule model of these workers, Parsons concludes that this cluster should have the three O's in a plane parallel to the electrode surface with the out of plane OH's oriented at 62° relative to this plane. The surface area of each such cluster should be $20A^2$.

Despite some degree of agreement between the Damaskin-Frumkin model and experiment, the source of the hump in the C vs. E curves and the high C values at anodic potentials is far from settled. Using a two-state model with individual water dipoles oriented towards or away from the surface, Bockris and Habib (43) have concluded that the solvent cannot be the source of the capacitance hump. Cooper and Harrison have also used a similar two-state model (47). More recently, Bockris and Habib (46) have extended their treatment to a three-state model by including a dimer-monomer equilibrium on the surface. Even with this model they still concluded that the capacitance hump is not the result of a solvent effect.

Several groups including Harrison et al. (44), Bockris and Habib (43, 46) and Reeves (45) have used the experimentally determined temperature dependence of the compact layer capacitance to show that the solvent surface excess entropy passes through a maximum at potentials or charge

slightly negative to the pzc (i.e., at a surface charge density of -4 to $-6\mu/cm^2$ (44)]. This is in a region where there are no special features to the capicatance vs. charge density or potneital plots. One could normally expect the maximum solvent polarizability to occur when the solvent at the interface has the maximum randomness and hence maximum entropy. This condition would in turn correspond to the maximum or hump in the capacitance vs. charge curves. Failure for this to be the situation is cited as strong evidence against solvent effects as responsible for the hump on the positive side of the pzc (43-46).

On the other hand, the Damaskin treatment (38) does yield a maximum in the $\partial(1/C)/\partial T$ vs. charge plot at small negative charge densities, rather close to that observed experimentally for Hg in aqueous NaF (see Fig. 7). Since the surface excess entropy of the solvent is calculated from $\partial(1/C)/\partial T$ as a function of charge density, it is expected that the Damaskin treatment should also lead to the observed maximum in the entropy at small negative charge densities.†

A distinct feature of the Damaskin-Frumkin and Parsons treatments is that they provide for changes in the surface concentration of water as well as orientational effects. These both contribute to the surface excess entropy and also the compact layer capacitance. The Bockris-Habib two and three-state models are such that only orientational contributions are included.

---

† Damaskin (38) points out, however, that a theory which accounts for the charge dependence of the surface excess entropy may not necessarily account for the temperature dependence of the compact layer capacitance. For example, the Bockris-Habib two-state model does describe reasonably well the surface excess entopy-charge density curves for Hg in aqueous NaF but at the same time predicts a negligible contribution of the solvent to the compact layer capacitance, and hence cannot describe C vs. T.

Those workers who are opposed to solvent effects as the explanation for the features of the C-q curves on the positive side of the pzc propose specific anionic adsorption as the cause (see e.g. 42-46), even with electrolytes involving F^- anions. With other anions such as Cl^-, Br^-, I^-, $SO_4^=$, ClO_4^- there is little question that specific adsorption does occur with the anion perturbing the compact layer. The F^- anion, however, has been presumed to be sufficiently strongly solvated that specific adsorption effects should be minor and probably negligible, at least until very anodic potentials relating to E_{pzc} are reached. Watts-Tobin (35) suggested that OH^- adsorption may occur at anodic potentials. In support of such specific anion effects, is the observation that additions of HF_2^- anions to a KF electrolyte produce substantial changes in the shape and position of the hump (48) (see Fig. 8). Various workers have attempted to correct the compact layer capacitance for specific anion adsorption (see e.g. 49,50) but it is not clear that the corrections are valid.

Capacitance measurements for Hg in various organic solvents show humps or maxima on the anodic side or cathodic side of the pzc or both (57). In some instances there is little doubt that the hump is the result of specific ionic adsorption because of the strong dependence on the type of anion. In other instances, specific anion adsorption is not a likely explanation.

It is quite evident that electrochemical methods alone are not able to resolve the question of the structure of the water layer adjacent to the metal electrode. The vibrational spectrum of this layer could be of immense help but neither infrared or Raman are promising because of the problem of distinguishing the properties of a monolayer of water in a sea of bulk water. Efforts have been made by Bewick and Robinson (52) to

obtain the optical constants of the water in the compact layer on lead and mercury using UV-visible reflectance spectroscopy but questions exist concerning their method for extracting information concerning the water layer from the reflectance data.

In the discussion so far, the electrode surface has been treated as a well-defined plane and the electronic properties of the electrode properties of the electrode plane not considered. The electronic properties of the electrode phase will be addressed by other speakers in conjunction with the interpretation of the optical properties. Even so, a qualitative description is desirable at this point to complete the discussion of the compact layer.

The truncation of the conduction band orbitals at the electrode surface results in an evanescent wave extending into the interface. When the charge on the metal q_m is changed, the extent to which the evanescent wave extends out from the metal surface changes, as shown in Fig. 9. The water dipoles and any ionic species in the inner Helmholtz plane feel this tail of this electron density decay curve. Even if there is no strong localized orbital interactions, their distance of approach will be influenced and the potential distribution across the compact double layer changed. Further, at high positive charge the extension of the evanescent wave out from the surface will be depressed. Under this circunstance, the s - conduction band electrons may no longer be as effective in shielding the more tightly bound d orbitals at the surface and specific interactions between the solvent and the d orbitals of the metal may become more probable. It is hoped that information concerning such interactions will be forthcoming from optical studies but so far, the electroreflectance data have yielded little new insight.

III. Adsorption at Electrochemical Interfaces

A. General features

With solid electrodes and probably even with liquid metals such as Hg, the understanding of the compact layer requires information concerning the possible adsorption sites for water and anionic species. With species that are strongly adsorbed and only weakly interact with other solutions phase species, it may be possible to gain insight into the most likely adsorption sites from theoretical and experimental studies of adsorption at single crystal solid-gas interraces. Many theorists are involved in efforts to calculate the heats of adsorption of hydrogen, oxygen, water, carbon monoxide and other species on various sites on metal surfaces using a variety of methods including LCAO, extended Hückel molecular orbital theory and Xα scattering. Leban and Hubbard (53) appear to be the first electrochemists to attempt to calculate such information for species of special interest to the understanding of the compact layer. Using the iterative extended Hückel molecular orbital technique, they have arrived at the preferred sites shown in Fig. 10 for various species on the Pt(III) surface. Aside from the limitations of the IEHMO teachnique, the calculation has other questionable features. Specific interactions of the adsorbed species with solution phase components are not considered; some are strong. Further, only five Pt atoms of the metal phase are included in the treatment (see Fig. 11). Even so, this calculation represents a first step for electrochemists.

With solid electrodes, the potential of zero charge and the double layer capacitance should be dependent on the surface orientation. Ample evidence exists for such dependence in the literature for metals (see e.q. 54-60) as well as graphite (61,62). In general the potential of zero charge appears to be most positive on the plane with the highest atom density for fcc metals such as Ag and Au.

B. Hydrogen electrosorption

Electrosorption plays a key role in electrocatalysis, a subject which has taken on new significance because of the world-wide energy problems. The adsorption of hydrogen is among the most important because of its involvement as an intermediates in a number of electrochemical processes. By far the most studied metal surface for hydrogen adsorption is platinum. Linear sweep voltammetry indicates a number of peaks (Fig. 12), whose potential and height are strongly dependent on the type of electrolyte. Conway et al. (64) have observed up to five peaks in sulfuric acid. Various explanations have been proposed including different adsorption sites on a given single crystal surface, a distribution of crystallographic surfaces, induced heterogeneity associated with hydrogen adsorption itself (64) and anion adsorption which induces heterogeneity by blocking sites to varying degrees and perturbing adjacent sites (63). The pronounced dependence of the hydrogen electrosorption on the type and concentration of anion (Fig. 12) indicates that hydrogen adsorption-desorption are coupled to anion desorption-adsorption (63).

In an attempt to resolve this problem, various electrochemists have examined hydrogen electrosorption on single crystal Pt. Will (65) examined the low index planes (100), (110) and (111) and found the same two major peaks on these three orientations although the relative heights depended on the crystal orientation. The single crystal Pt electrodes studied by Will probably did not expose a single crystallographic surface. The distribution of crystallographic surface planes depends on the overall orientation and the extent to which the surface has been cycled to anodic potentials. Will arrived at the conclusion that the strongly adsorbed hydrogen peak IV (Fig. 12) corresponds to the 100 plane and the weakly adsorbed peak I to the (110) plane. Rather analogous results have been reported by Bronel et al.(66) for the Pt (100) and (111) surfaces. These workers used electron microscopy to establish that the surfaces were facet-free. Kinoshita and Stonehart(67) have examined hydrogen adsorption on dispersed Pt as a function of crystallite size and find a dependence which they interpret as further evidence that the multiple peaks result from different surface crystallographic structures.

In contrast, Bagotzky et al. (68) and Conway et al. (64) have concluded from their single crystal Pt studies that there is little difference in the hydrogen adsorption on the (100) (110) and (111) planes. Conway et al. (64) attribute the multiple peaks principally to induced heterogeneity arising from collective long-range electronic interactions.

The probability is high in all of the single crystal studies just cited that the surface prevailing during the electrochemical measurements

does not correspond to a single crystal plane. Even if the Pt crystal has only one plane predominant before the electrosorption measurement, these authors generally cycled their electrodes to anodic potentials in the anodic film region to oxidize or desorb interfering surface contaminants and this procedure is likely to cause restructuring.

Recently several groups have attempted to devise techniques which permit the introduction of a single crystal surface of predominantly one plane and free of impurities into an electrochemical environment with a minimum possibility of restructuring and contamination. These include A. Hubbard at the University of California at Santa Barbara(16,18), J. A. Joebstl at Fort Belvoir (19), P. N. Ross at United Technology (20) and the author's group at Case Western Reserve University (17,21). Each group has turned its attention to the (100), (11) and (111) planes of Pt and first establishes that the surface is predominantly one plane using low energy electron diffraction (LEED) and free of surface impurities down to a few percent of a monolayer using Auger electron Spectroscopy.

The key features of the techniques used by the author's group (75) are vacuum transfer with 99.9999% argon admitted to the vacuum systems just prior to the electrochemical measurements; thin-layer electrochemical cell techniques to avoid contamination; and introduction of the Pt single crystal surfaces into the electrolyte at controlled potentials in the hydrogen adsorption region. In the cyclic voltammetry studies of hydrogen electrosorption, the potential range is restricted to +0.05 to 0.40 V vs RHE to reduce any possible restructuring. The voltammetry curves on the single

crystal Pt surfaces retract with repeated cycling, starting with the very first sweep. If the voltage sweep is extended into the anodic film formation region to $\geq$ 1.4V vs. RHE, the hydrogen adsorption region changes significantly with new peaks appearing or very minor peaks becoming major peaks, depending on the original surface. This is probably the result of restructuring although the possibility exists that oxygen has been irreversibly adsorbed into sites within the surface layer.

On the Pt (100) surface, Hubbard et al. (18), Ross (20) and our group (21) find one predominant peak (Fig. 13) corresponding to the strongly adsorbed hydrogen peak on polycrystalline Pt in acid solutions. The LEED pattern for the Pt (100 indicates a 5 x 1 overlayer mesh (15,21). This surface probably reverts to (1x1) in contract with the electrolyte. On the Pt (111) surface, our group finds only a minor peak corresponding to weakly adsorbed hydrogen while Ross and Hubbard et al. report a major peak. The source of this discripancy is not fully clear but may be caused by exposure to or cycling of the electrode to potentials in the anodic film region by the other groups. Alternatively our Pt (111) surface might have some of the sites blocked by an impurity but Auger does not indicate any such impurity. In any event, the presence of only one major peak on the (100)Pt surface provides strong evidence that the principal peaks on polycrystalline Pt correspond to different crystallographic planes.

Hydrogen adsorption has been studied on polycrystalline Pt electrodes using UV-visible reflectance spectroscopy by McIntyre and

Kolb (69) and Bewick and Tuxford (70). The strongly bound hydrogen (Peak IV in Fig. 12) produces only a small reflectance increase at 435 nm while the weakly bound component (Peak I) produces a larger reflectivity decrease (70). The means by which the hydrogen adsorption produces these optical changes have not yet been established. The effect may be caused principally by changes in the surface conductivity rather than by the chemical bonding itself.

C. Underpotential electrodeposition of other species.

Various metal cations electrodeposit on foreign metal substrates in mono-and submonolayers at potentials far below the reversible potentials for electrodeposition of the bulk metals. UPD is of considerable interest to electrochemists because of the importance of such layers to the understanding of electroplating (78) as well as the interesting electrocatalytic properties of such layers (e.g. 79,80). These layers range from principally ionic to metallic depending on the particular solution phase species, substrate, coverage and potential. This phenomenon resembles somewhat the adsorption of metal atoms from the gas phase on foreign metal substrates (see e.g. 81-85) except that the solvent (particularly water) at the interface tends to enhance the ionic character of the bonding of the adsorbate to the metal substrate. Field emission studies (e.g. 86-87) have helped to identify the nature of the electronic interactions for such layers on metals in vacuo. Quantum mechanical models have been developed for the interaction of the valency orbitals of the adsorbed species with the conduction and valence bands of the metal substrate (e.g. 88). LEED studies have indicated ordering in some such monolayers (e.g.83). Unfortunately such information can not be translated to the corresponding

electrochemical interface because the interactions with solvent are expected to be strong in many instances. Various electrochemical methods (for a review see ref. 89) have been used to obtain information concerning coverage and the charge supplied to the electrode but have yielded little atomic level information concerning the absorbate-substrate bonding. Bowles and Cranshaw (90) have obtained in situ Mössbauer data for Sn on Pt, indicating metallic character for the UPD layer but Mössbauer spectroscopy is quite limited in its applicability. The principal spectroscopic tool has been UV-visible reflectance spectroscopy (76,91-94), including ellipsometry (77). The optical data carry quantitative information concerning the surface interactions involved in UPD but the interpretation of such data is still in a very qualitative state (9).

The various features of UPD are well illustrated by Pb on Au substrates. Figures 14 and 15 indicate the current-voltage curves for the adsorption and desorption of Pb species during linear voltage sweeps for vapor deposited polycrystalline and single-crystal Au substrates. Conway (95) has resolved 7 peaks for the UPD of Pb on polycrystalline Au. The substrate morphology has a pronounced effect on these voltammetry curves as well as the charge-potential curves (Fig. 16). Similar effects have been reported for other cations on single crystal Au by Schultze and Dickertmann (71). The peaks in the voltammetry curves are accompanied by relatively large changes in the reflectivity and ellipsometric parameters (77).

The widths of the voltammetry peaks attending the adsorption and desorption of a solution phase species depend on the heterogeneity

of the surface and the interactions between adjacent species in the UPD layer and also the water molecules at the interface. Attractive interactions between the adsorbed species cause the peak to narrow down. The sharp peak at + 0.050V vs SHE in Fig. 14, however, is extremely narrow and has fine structure which is not fully resolved. The effects of sweep rate and electrolyte concentration (83) indicate that this peak does not correspond to adsorption-desorption but rather a transition within the UPD layer involving a change in the surface charge. This change might be an order-disorder transition of the type observed with adsorbed layers at metal-vacuum interfaces. On the other hand, the change in charge attending this peak is large (see Fig. 16), and further, the ellipsometric measurements indicate a pronounced change to a more metallic-like layer (84). It has been proposed (76) that this peak corresponds to a phase transition in which the adsorbed Pb species with significant ionic character condense into metallic patches. The situation may be represented as follows

a. $$Pb^{2+}_{aq} + (2-y)e^- \rightleftharpoons Pb^{y+}_{ads}$$

b. $$Pb^{y+}_{ads} + ye^- \rightleftharpoons Pb_{ads}$$

where Reaction a corresponds to the more anodic voltammetry peaks and Reaction b to the very sharp peak in Fig. 14. Unfortunately it is not possible to measure directly y in Reactions a and b since the charge passed through the external circuit includes the charge necessary to

compensate changes in the ionic double layer.

A probable model for the interactions of the adsorbed Pb with the Au substrate and other adsorbed lead ions or atoms is presented in Fig. 17 A and B for low moderate coverage where the lead is ionic and in Fig. 17 C and D for high coverage where the Pb is metallic. The representation is that usually employed for adsorption at metal-gas interfaces (see e.g. 87) and makes no attempt to show solvent states. Further, these figures are applicable at or near the point of zero charge (pzc) where the potential gradients associated with differences in the potentials of the metal and solution phases are small compared with those intrinsic to the electronic structure of the interface. Figures 17A and C represent the potential energy profiles perpendicular to the surface through the center of a Pb ion or atom while Fig. 17 B and D represent the corresponding profiles parallel to the surface through the center of nearest neighbor Pb ions or atoms. The dashed lines represent the potential energy of an electron when there is no interaction, electrostatic or otherwise, between the Au and Pb. The solid curves are the combined potential energy curves.

In Fig. 17 A and C the potential energy curve between the metal surface and the Pb is lowered near the intersection of the two separate curves by resonance splitting. At high coverages, this resonance splitting is much larger than at low coverages because the three-dimensional aspect of Pb-Pb as well as Pb-Au interactions becomes important.

In Fig. 17 A the valence orbitals (6p) of the adsorbed Pb are broadened through interaction with the orbitals of the Au with part of the Pb valence orbital band below the Fermi level. This results in

a charge on the adsorbed Pb of less than +2. The depression of the potential energy barrier between the Pb and Au, however, is assumed not to be sufficent to reduce the top of the barrier below the Fermi level and thus in this case, the Pb-Au interaction is not yet metal-liclike. The possibility that the barrier has been pulled down below the Fermi level, even at low coverages, cannot be ruled out at this time, but this is unlikely without the three-dimensional interactions within the layer as well as between the layer and the substrate.

Such three-dimensional interactions are to be expected at high coverages. In Fig. 17 C and D, the barriers are shown depressed below the Fermi level, i.e., the lead layer is metallic. The phase transition to which the sharp Pb voltammetry peak is ascribed serves to bring the Pb species into the close proximity required to achieve metallic properties for the layer.

The potential energy plots in Fig. 17 will change with electrode potential, at least qualitatively, in a manner similar to that used to represent the situation in field emission at metal-vacuum interfaces (87). In Fig. 17 A,the barrier will be lowerd as the electrode potential is driven cathodic. Once the barrier falls below the Fermi level, however, the fraction of the electrode potential difference felt by this barrier will become very small because of the metallic properties of the Pb and the smallness of the Thomas-Fermi screening distance.

Conclusion: This discussion indicates that the electrochemist has very little quantitative understanding of his interfaces and that even his qualitative models are often in doubt. Hopefully in situ optical methods combined with theoretical methods will lead to new insight into the nature of electrochemical interfaces.

Acknowledgement: The preparation of this paper has been made possible through research support from the U.S. Office of Naval Research.

REFERENCES

1. C. A. Barlow, Jr., "The Electrical Double Layer," in Physical Chemistry, An Advanced Treatise, Vol. IXA, Chapter 2, H. Eyring, D. Henderson and W. Jost, eds., Academic Press, New York City, 1970.

2. C. A. Barlow, Jr., and J. R. Macdonald, "Theory of Discreteness of Charge Effects in the Electrolyte Compact Double Layer," in Advances in Electrochemistry and Electrochemical Engineering, P. Delahay and C. Tobias, eds., J. Wiley and Sons, New York, 1967.

3. R. Payne, J. Electroanal. Chem., 41, 277 (1973).

4. W. Lorenz, Z. Phys. Chem., 248, 161 (1971); 252, 374 (1973); 253, 243 (1973).

5. K. J. Vetter and J. W. Schultze, Ber. Bunsenges. Phys. Chem., 76, 920 (1972).

6. J. W. Schultze and K. J. Vetter, J. Electroanal. Chem., 44, 63 (1973); 53, 67 (1974); Electrochim. Acta, 19, 230 (1974).

7. J. W. Schultze and F. D. Koppitz, Electrochim. Acta, 21, 327 (1976).

8. A. Frumkin, B. Damaskin and O. Petrii, J. Electroanal. Chem., 53, 57 (1974); Elektrokhim., 12, 1 (1976).

9. J.D.E. McIntyre in "Optical Techniques in Electrochemistry", Vol. 9, R. H. Muller, ed., Advances in Electrochemistry and Electrochemical Engineering, J. Wiley and Sons, New York City, 1973.

10. G. Blondeau and E. Yeager, Progress in Solid State Chemistry, 11, 153 (1976).

11. A. Reed and E. Yeager, Electrochim. Acta, 15, 1345 (1970).

12. D. Laser and M. Ariel, J. Electroanal. Chem., 41, 381 (1973).

13. (a) M. Fleischmann, P. Hendra and A. J. McQuillan, Chem. Phys. Letters, 26, 163 (1974).
    (b) A. J. McQuillan, P. J. Hendra and M. Fleischmann, J. Electroanal. Chem., 65, 933 (1975).
    (c) R. P. Cooney, E. S. Reid, P. J. Hendra and M. Fleischmann, J. Amer. Chem. Soc., 99, 2002 (1977).

14. R. P. Van Duyne, D. L. Jeanmaire, M. R. Suchanski, W. Wallace and T. Cape, "Resonance Raman Spectroelectrochemistry", National Meeting, The Electrochemical Society, Washington, D.C., May 1976, Paper 357. (Extended Abstracts, pp. 883-4).

15. G. Hagen and E. Yeager, unpublished data for electrosorbed p-nitroso-dimethyl aniline; to be submitted for publication.

16. R. M. Ishikawa and A. T. Hubbard, J. Electroanal. Chem., 69, 317 (1976).

17. W. E. O'Grady, M.Y.C. Woo, P. L. Hagans and E. Yeager, J. Vac. Sci. Technol., 14, 365 (1977).

18. A. T. Hubbard, J. A. Schoeffel and H. W. Walter, "Ethylene Hydrogenation and Related Reactions on Single Crystal and Polycrystalline Pt Electrodes",

National Meeting, American Chemical Society, New Orleans, Mar. 1977, Paper COLL-142.

19. J. A. Joebstl, "Surface Characterization of Electrocatalysts by LEED, Auger Electron Spectroscopy and Related Techniques", First Chemical Congress of North American Continent, Mexico City, Nov. 30-Dec. 5, 1975. Paper PHSC-18.

20. P. N. Ross, "Electrocatalytic Properties of Single Crystal Pt Surfaces in Aqueous Acid Electrolytes", in Proceedings of the Symposium on Electrode Materials and Processes for Energy Conversion and Storage, National Meeting, The Electrochemical Society, Philadelphia, May 8-13, 1977, Paper 343. (Extended Abstracts pp. 878-880).

21. W. E. O'Grady, M.Y.C. Wood, P. L. Hagans and E. Yeager, "Electrochemical Hydrogen Adsorption on the Pt (111) and (100) Surfaces", loc. cit., Paper 335 (Extended Abstracts, pp. 859-861).

22. J. O'M. Bockris, M. A. Devanathan and K. Muller, Proc. Roy. Soc. A274, 55 (1963).

23. H. L. Friedman, "Ionic Solution Theory Based on Cluster Expansion Methods", J. Wiley and Sons, New York, 1962.

24. N. F. Mott and R. J. Watts-Tobin, Electrochim. Acta, 4, 79 (1961).

25. H. Brodowsky and H. Strehlow, Z. Elektrochem. 63, 262 (1959).

26. J. R. Macdonald, J. Chem. phys., 22, 1857 (1954).

27. G. Lippmann, Ann. chim. phys., 5, 494 (1875).

28. V. S. Krylov and V. G. Levich, Zhur. Fiz. Khim., 37, 106, 2273 (1963).

29. V. G. Levich and V. A. Kir'yanov, Doklady Akad. Nauk SSSR, 131, 1134 (1960).

30. F. B. Buff and F. H. Stillinger, J. Chem. Phys., 39, 1911 (1963).

31. O. A. Esin and B. F. Markov, Zhur. Fiz. Khim., 13, 318 (1939).

32. D. C. Grahame, Z. Elektrochem., 62, 264 (1958).

33. D. C. Grahame, J. Amer. Chem. Soc., 76, 4819 (1954).

34. J. R. Macdonald and C. A. Barlow, J. Chem. Phys., 36, 3062 (1962).

35. R. J. Watts-Tobin, Phil. Mag., 6, 133 (1961).

36. S. Levine, G. Bell and A. Smith, J. Phys. Chem., 73, 3534 (1969).

37. B. B. Damaskin and A. N. Frumkin, Electrochim. Acta, 19, 173 (1974).

38. B. B. Damaskin, J. Electroanal. Chem., 75, 359 (1977).

39. R. Parsons, ibid., 59, 229 (1975).

40. D. C. Grahame, J. Amer. Chem. Soc., 79, 2093 (1957).

41. J. Del Bene and J. A. Pople, J. Chem. Phys., 52, 4858 (1970).

42. R. Payne, J. Electroanal. Chem., 41, 309 (1973).

43. J. O'M. Bockris and M. A. Habib, ibid., 65, 473 (1975).

44. J. A. Harrison J.E.B. Randles and D. J. Scheffrin, ibid., 48, 359 (1973).

45. R. N. Reeves in Modern Aspects of Electrochemistry, Vol. 9, J. O'M. Bockris and B. E. Conway, eds., Plenum Press, New York, 1974.

46. J. O'M. Bockris and M. A. Habib, Electrochim. Acta, in press.

47. I. L. Cooper and J. A. Hanson, J. Electroanal. Chem., 66, 85 (1975).

48. A. W. Verkroost, M. Sluyters-Rehbach and J. H. Sluyters, ibid., 24, 1 (1970).

49. R. Payne, J. Electrochem. Soc., 113, 999 (1966).

50. R. Payne, Trans. Faraday Soc., 64, 1638 (1968).

51. R. Payne, "The Electrical Double Layer in Non-aqueous Solutions", in Advances in Electrochemistry and Electrochemical Engineering, Vol. 7, P. Delahay and E. Tobias, eds., J. Wiley and Sons, New York, 1970.

52. A. Bewick and J. Robinson, J. Electroanal. Chem., 71, 131 (1976), ibid. 60, 163 (1975).

53. M. A. Leban and A. T. Hubbard, J. Electroanal. Chem., 74, 253 (1976).

54. A. Hamelin and G. Valette, Compt. rend., 269C, 1020 (1969).

55. T. Vitanov, E. S. Sevast'yanov, V. Bostanov and E. Budewski, Elektrokhim., 5, 451 (1969).

56. R. D. Giles and J. A. Harrison, J. Electroanal. Chem., 24, 399 (1970).

57. J. W. Diggle and B. Lovrecek, ibid., 24, 119 (1970).

58. A. Hamelin and J. Lecoeur, Coll. Czech. Chem. Comm., 36, 714 (1971).

59. N. V. Huong and J. Clavilier, Compt. rend., 272C, 1404 (1971).

60. A. Hamelin and P. Dechy, ibid., 272C, 1450 (1971).

61. J. P. Randin and E. Yeager, J. Electrochem. Soc., 118, 711 (1971).

62. J. P. Randin and E. Yeager, J. Electroanal. Chem., 36, 257 (1972).

63. J. C. Huang, W. E. O'Grady and E. Yeager, J. Electrochem. Soc., in press.

64. H. Angerstein-Kozlowska, W.B.A. Sharp and B. E. Conway, in Proceedings of the Symposium on Electrocatalysis, M. W. Breiter, ed., The Electrochemical Society, Princeton, N.J., 1974, p. 94.

65. F. Will, J. Electrochem. Soc., 112, 451 (1965).

66. G. Bronel, M. Haim, J. Pesant and G. Peslerbe, Surface Sci., 61, 297 (1976).

67. K. Kinoshita and P. Stonehart, Electrochim. Acta, 20, 101 (1975).

68. V. S. Bagotszky, Yu. B. Vassiliev and J. I. Pyshnograeva, Electrochim. Acta, 16, 2141 (1971).

69. J.D. E. McIntyre and D. M. Kolb, Symp. Faraday Soc., 4, 99 (1970).

70. A. Bewick and A. M. Tuxford, ibid., 4, 114 (1970).

71. J. W. Schultze and D. Dickertmann, Surface Sci. 54, 489 (1976).

72. D. M. Kolb, M. Przasnyski and H. Gerischer, J. Electroanal. Chem., 54, 25 (1974).

73. V. A. Vicente and S. Bruckenstein. Anal. Chem. 45, 2036 (1973).

74. G. W. Tindall and S. Bruckenstein, Electrochim. Acta 16, 245 (1971).

75. H. Gerischer, D. M. Kolb and M. Przasnyski, Surface Sci. 43, 662 (1974).

76. R. Adzic, E. Yeager and B. D. Cahan, J. Electrochem. Soc. 121, 474 (1974); 121, 1611 (1974).

77. J. Horkans, B. D. Cahan and E. Yeager, ibid. 122, 1585 (1975).

78. D. J. Astley, J. A. Harrison and H. R. Thirsk, J. Electroanal. Chem. 19, 325 (1968).

79. R. R. Adzic and A. R. Despic, J. Chem. Phys. 61, 3482 (1974).

80. R. R. Adzic, D. N. Simic, D. M. Drazic and A. R. Despic, J. Electroanal. Chem. 61, 117 (1975).

81. R. L. Gerlach and T. N. Rhodin, Surface Sci. 17, 32 (1969); 19, 403 (1970).

82. J. Polanski and Z. Sidorski, Surface Sci. 40, 282 (1973).

83. J. Henrion and G. E. Rhead, Surface Sci. 29, 20 (1972).

84. J. Perdereau and J. Szymerska, Surface Sci. 32, 247 (1972).

85. F. Delamare and G. E. Rhead, Surface Sci. 35, 172 (1973).

86. L. D. Schmidt and R. Gomer, J. Chem. Phys. 42, 705 (1970).

87. J. W. Gadzuk, Phys. Rev., B, 1, 2110)1970).

88. J. W. Gadzuk, Surface Sci. 6, 133 (1967).

89. W. Lorentz, H. Hermann, N. Würthrich and F. Hilbert, J. Electrochem. Soc. 121, 1167 (1974).

90. B. J. Bowles and J. E. Cranshaw, Phys. Letters 17, 258 (1965).

91. T. Takamura, K. Takamura, W. Nippe and E. Yeager, J. Electrochem. Soc. 117, 626 (1970).

92. J.D.E. McIntyre and D. M. Kolb, Symp. Faraday Soc. 4, 99 (1970).

93. D. M. Kolb, D. Leutloff and M. Przasnyski, Surface Sci., 47, 622 (1975).

94. T. Takamura, Y. Sato and K. Takamura, J. Electroanal. Chem., 11, 31 (1973).

95. B. E. Conway, in "Electrocatalysis on Non-Metallic Surfaces", NBS Special Publication 455, U.S. Dept. of Commerce, Washington, 1976, pp. 107-124.

Table 1. *In situ* optical spectroscopic techniques for the study of electrochemical interfaces

1. specular reflectance spectroscopy and ellipsometry: external, internal
2. diffuse reflectance spectroscopy
3. transmission spectroscopy (transparent substrates)
4. Raman (including resonant Raman)
5. surface Brillouin
6. photo-acoustical spectroscopy
7. photon assisted charge transfer

Table 2. Types of information from optical studies of electrochemical interfaces

1. electronic surface properties: metal and semiconductor electrodes

2. adsorption of electrolyte phase species

   a. type of bonding
   b. adsorption isotherms
   c. adsorption kinetics

3. passivation layers

   a. structure, thickness
   b. kinetics of formation and reduction

4. battery cathodes: valency state-composition information

5. reaction intermediates: identification and quantitative analysis

6. identification of surface groups attached to the electrode surface (e.g., carbons, graphites, compound semiconductors, derivatized-chemically modified surfaces)

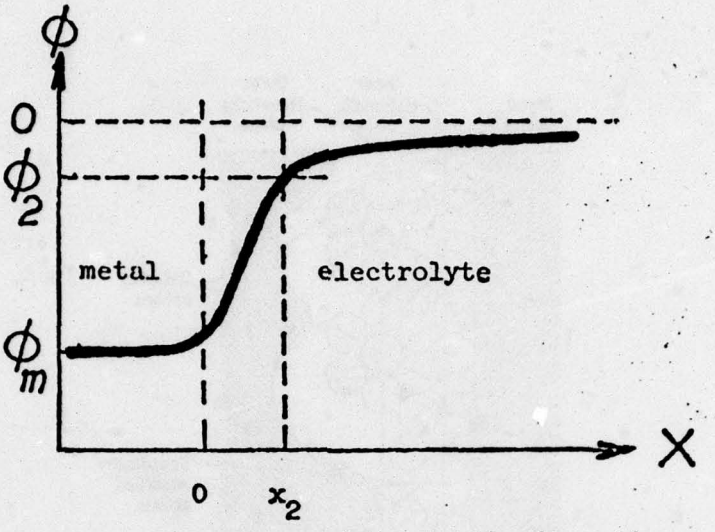

a. without specific ionic adsorption

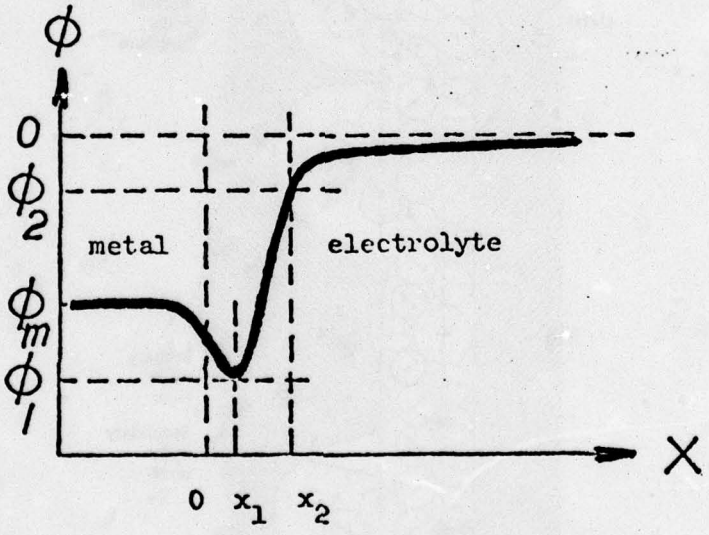

b. with specific ionic adsorption

Figure 1. Potential distribution across the electrochemical surface and without ionic specific adsorption. Region I: Helmholtz layer (compact). Region II: Gouy-Chapman layer (diffuse).
x_2-distance of closest approach without specific adsorption.
x_1-distance of closest approach of specifically adsorbed ion.

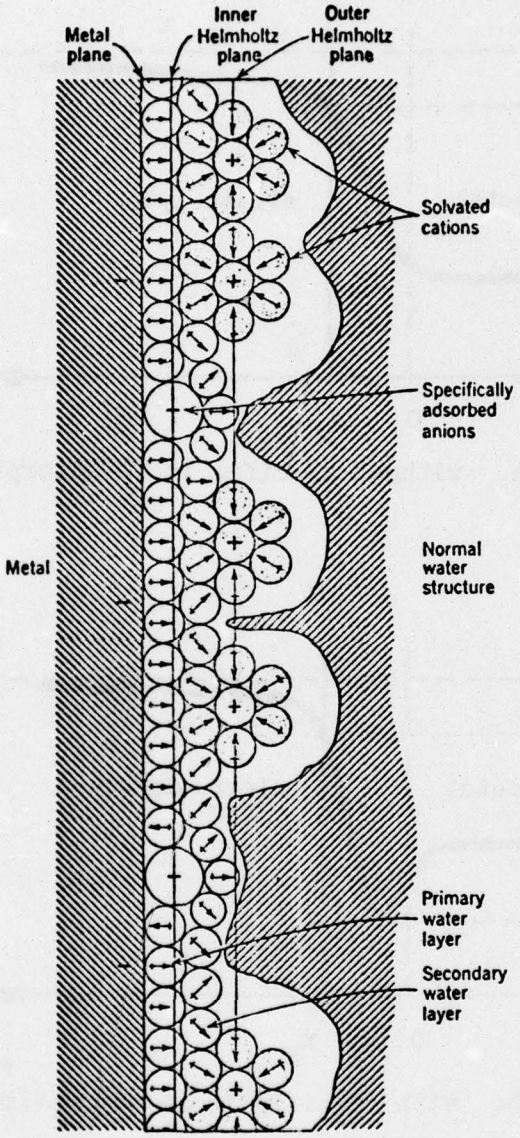

Figure 2. Model for ionic double layer of Bockris, Devanathan and Muller (22).

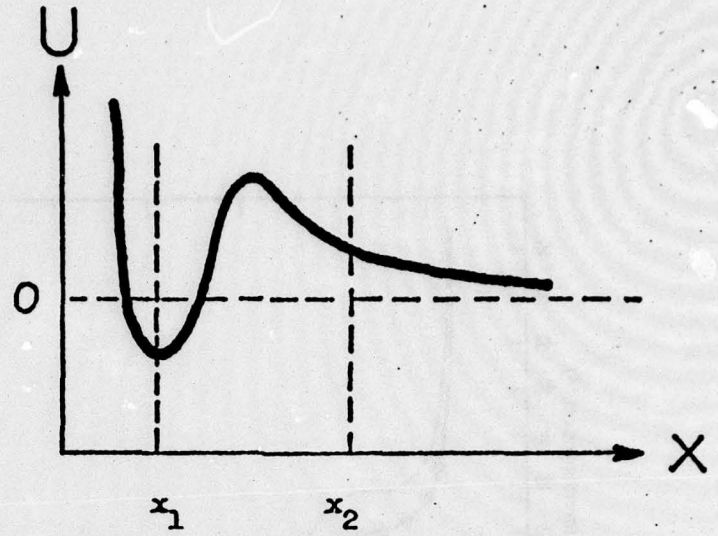

a. without specific ionic adsorption

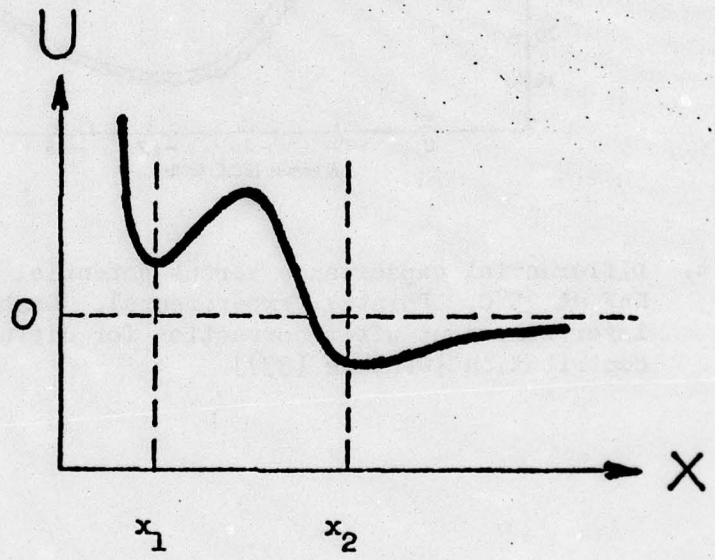

b. with specific ionic adsorption

Figure 3. Potential energy versus distance for anions and cations corresponding to Fig. 2.

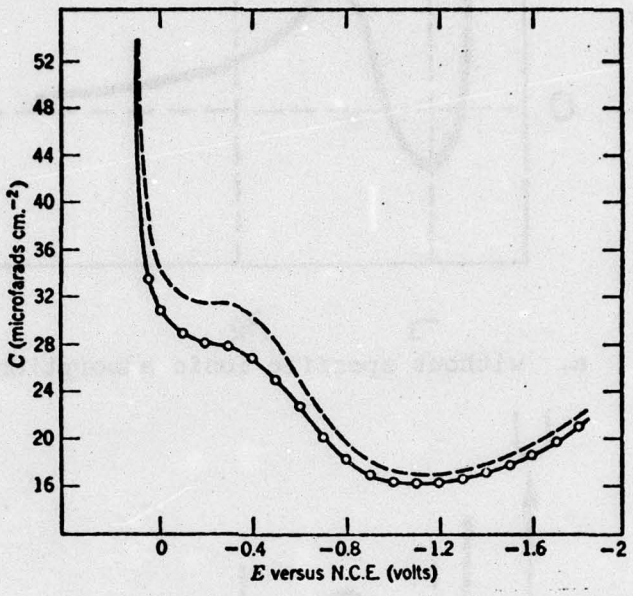

Figure 4. Differential capacitance versus potential for Hg in 0.916 M NaF at 25°C. Points: experimental. Dashed line: compact layer component after correction for diffuse layer contribution [Grahame (33)].

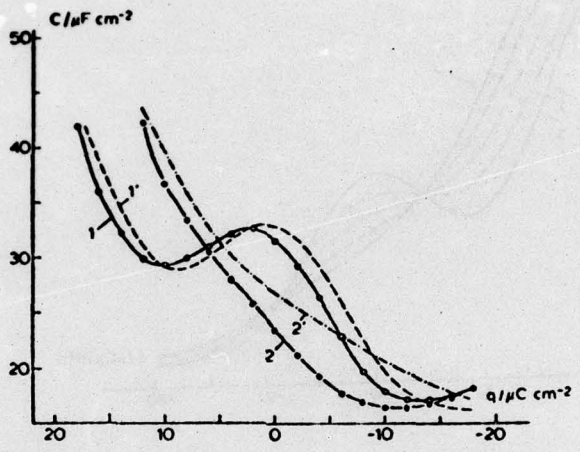

Figure 5. Compact layer capacitance versus charge according to Damaskin (38). Solid lines and points correspond to experimental data of Grahame (40) for Hg in aqueous NaF. Dashed line corresponds to theoretical. Curves 1, 1′: 0°C. Curves 2, 2′: 84°C. Consult ref. 38 for various parameters used in calculating the theoretical curves. (n_o = 3, n_{85} = 2, λ = 1). [Damaskin (38)].

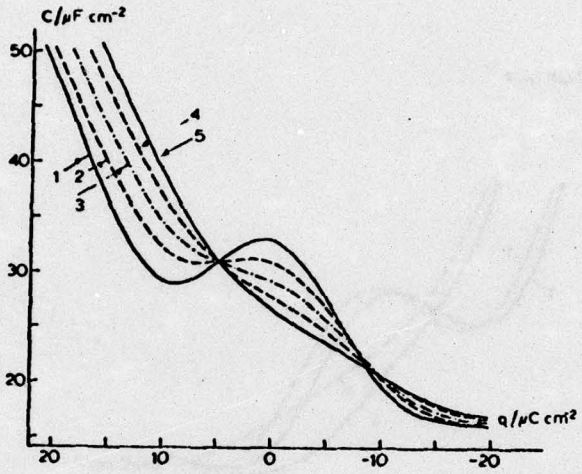

Figure 6. Compact layer capacitance versus charge density at various temperatures as calculated by Damaskin (38). Temperatures: 1) 0°C, 2) 25°C, 3) 45°C, 4) 65°C, 5) 85°C. Various parameters are the same as for Fig. 5 [Damaskin (38)].

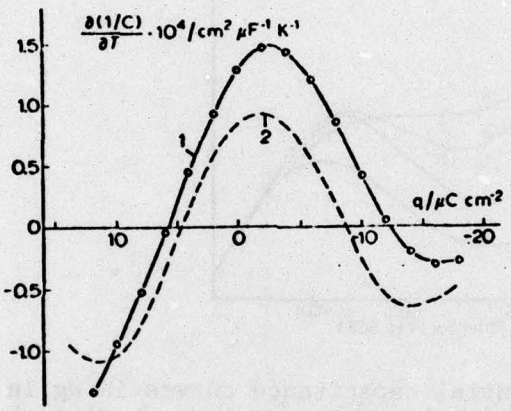

Figure 7. Dependence of d(1/C)/dT on charge density. Curve 1: calculated from Grahame's experimental data (40) for Hg in aqueous NaF. Curve 2: calculated from theoretical curves in Fig. 6 [Damaskin (38)].

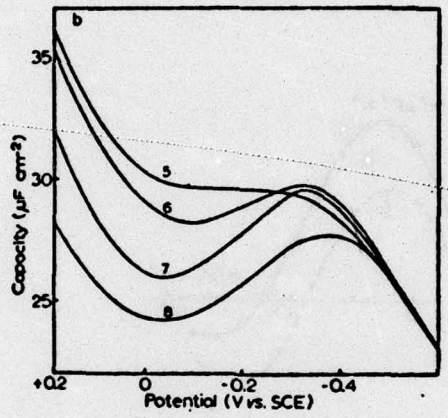

Figure 8. Differential capacitance curves in Hg in xM KF + (1-x) M KHF_2. Values x: 5) 0.94; 6) 0.68; 7) 0.35; 8) 0.14. [Verkroost et al. (48)].

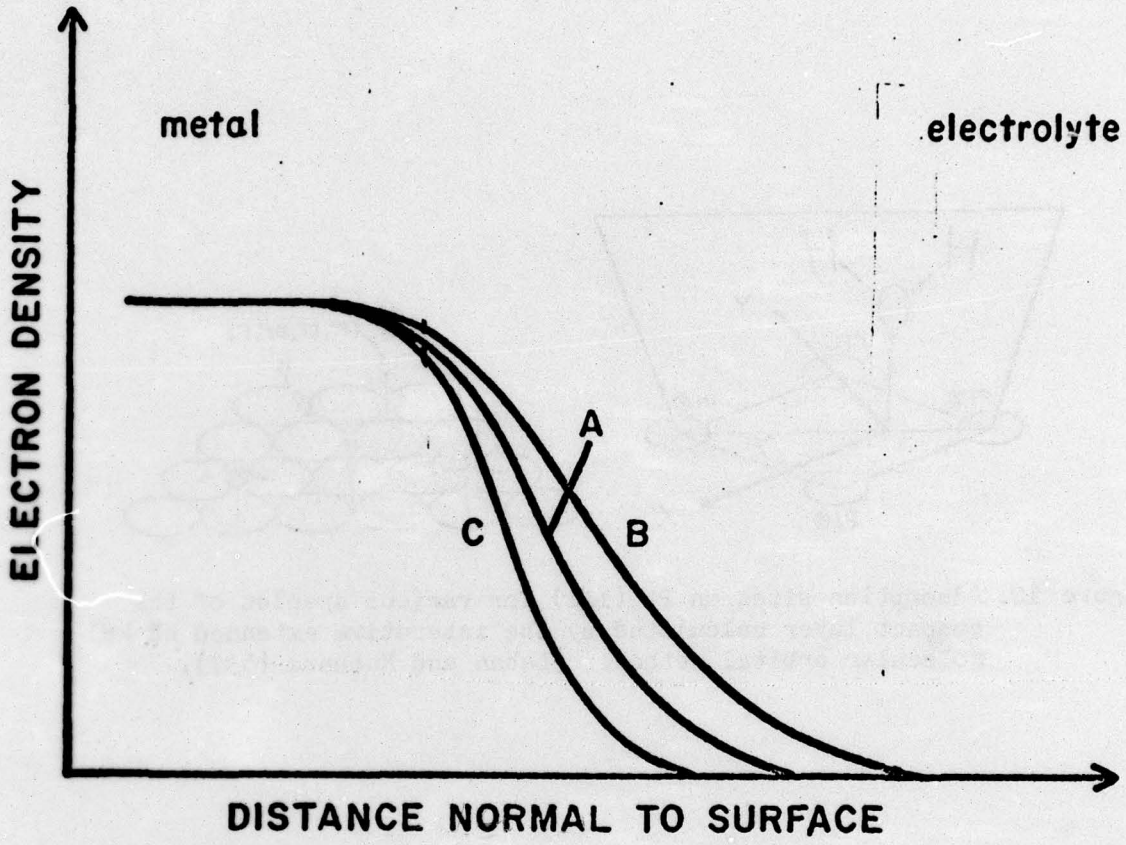

Figure 9. Electron density versus distance at a metal electrode surface. Curve A: at potential of zero charge (pzc). Curve B: cathodic to pzc. Curve C: anodic to pzc.

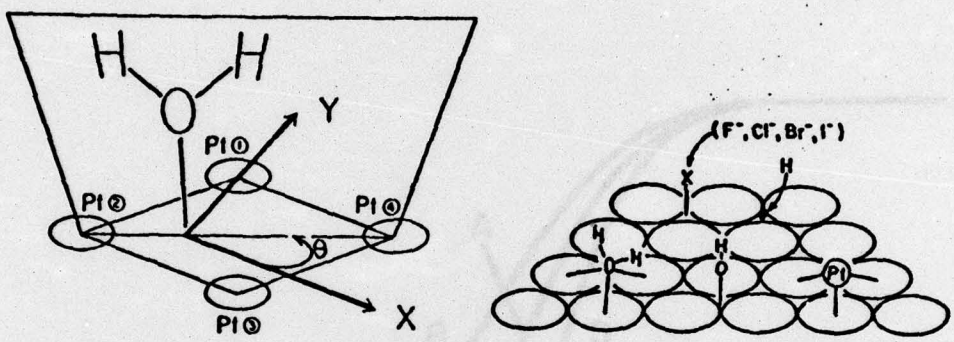

Figure 10. Adsorption sites on Pt (111) for various species of the compact layer calculated by the interative extended Hückel molecular orbital method. [Leban and Hubbard (53)].

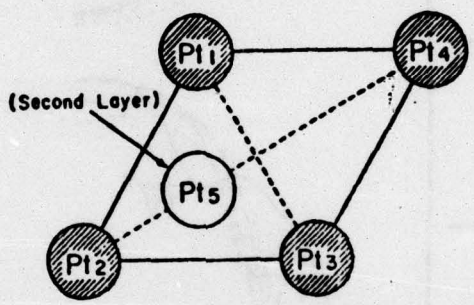

Figure 11. Model of Pt (111) surface used by Leban and Hubbard in the IEHMO treatment of adsorbed species. Shaded circles: atoms in the surface layer. Open circles: an atom in the second layer.

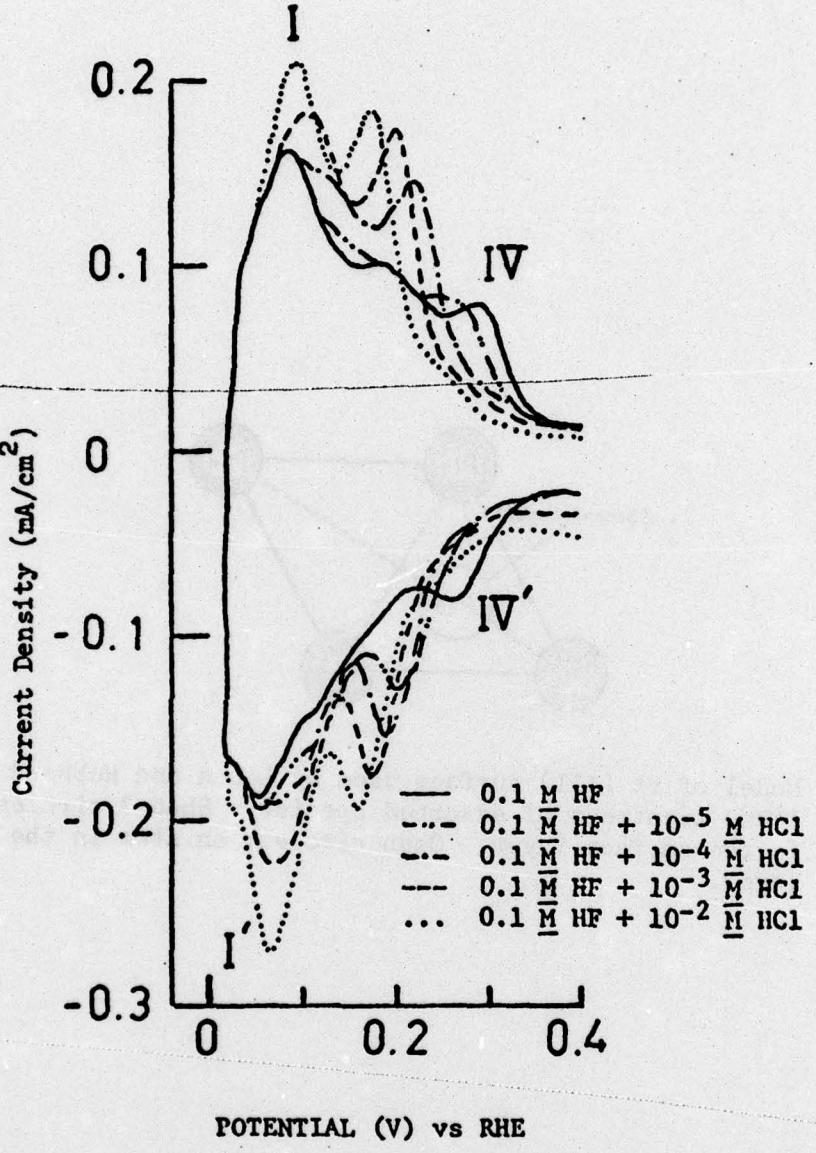

Figure 12. Voltammograms for hydrogen adsorption-desorption on polycrystalline Pt in 0.1M HF with various HCl additions. [Huang, O'Grady and Yeager (63)].

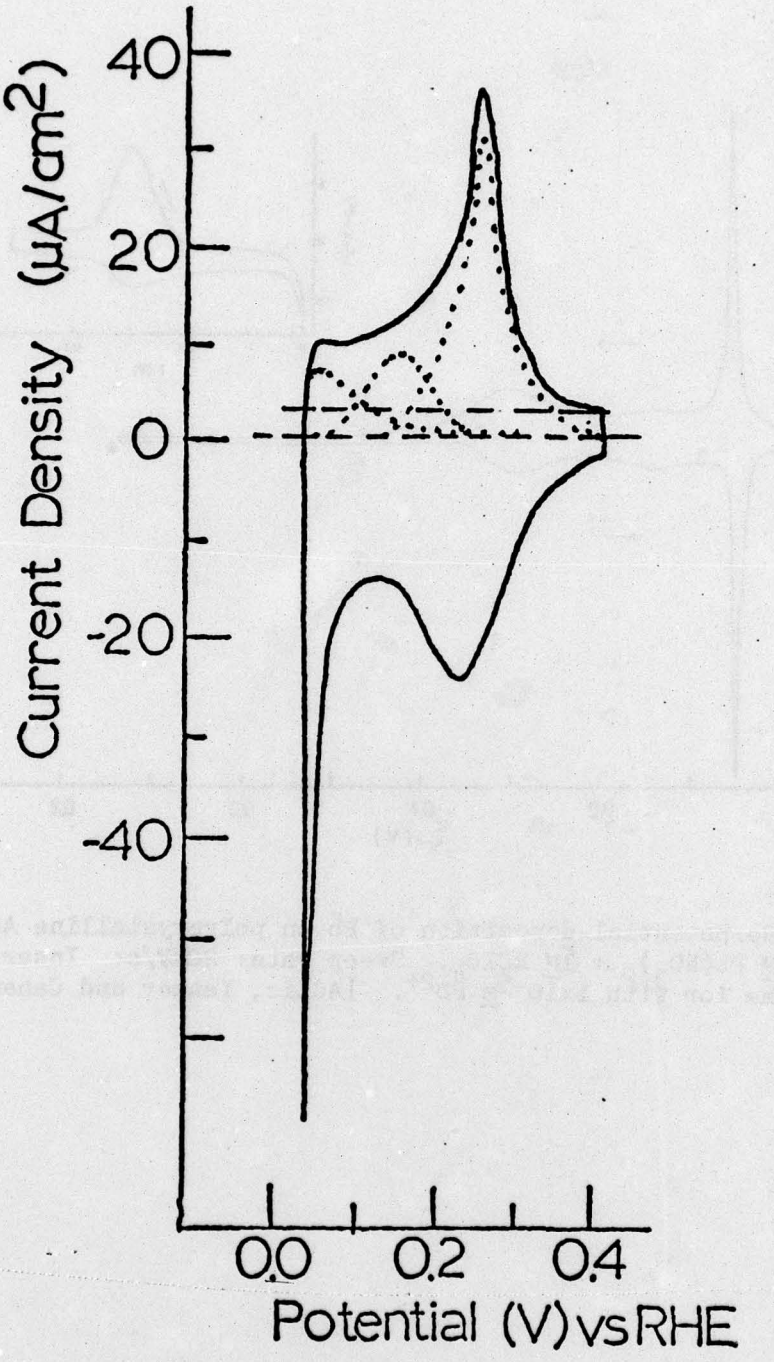

Figure 13. Voltammogram for hydrogen adsorption-desorption on clean Pt (100-5x1) in 0.05M H_2SO_4. Sweep rate: 50mV/s [O'Grady, Woo, Hagans and Yeager (74)].

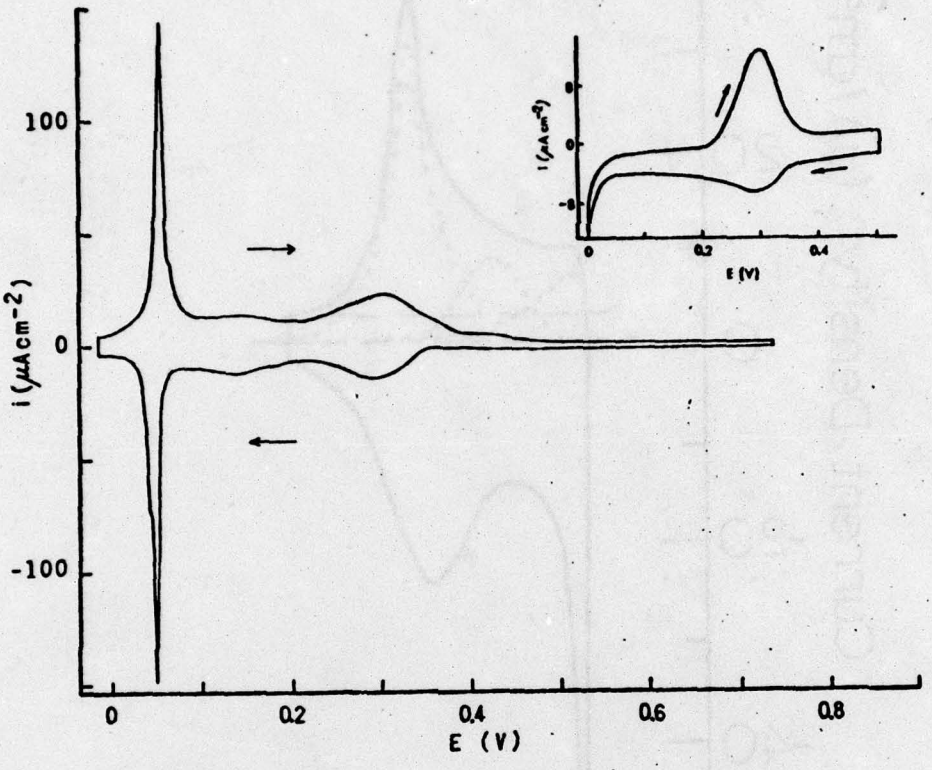

Figure 14. Underpotential deposition of Pb on polycrystalline Au in 1m$\underline{M}$ $Pb(NO_3)_2$ + 1$\underline{M}$ $HClO_4$. Sweep rate: 20mV/s: Insert: beha ior with $1x10^{-5}\underline{M}$ Pb^{2+}. [Adzic, Yeager and Cahan(76)].

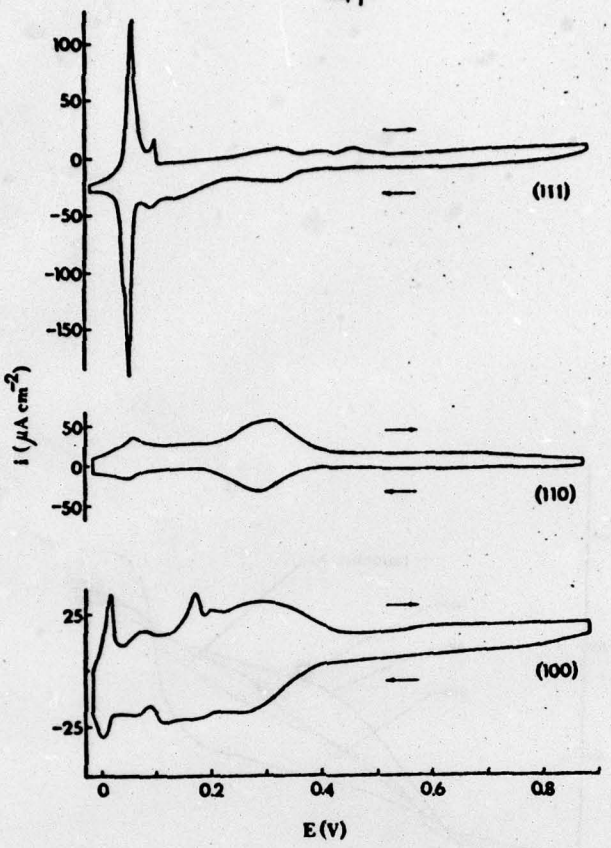

Figure 15. Underpotential deposition of Pb on single crystal Au in 1m$\underline{M}$ $Pb(NO_3)_2$ + 1$\underline{M}$ $HClO_4$. Sweep rate: 20mV/s [Adzic, Yeager and Cahan[76]].

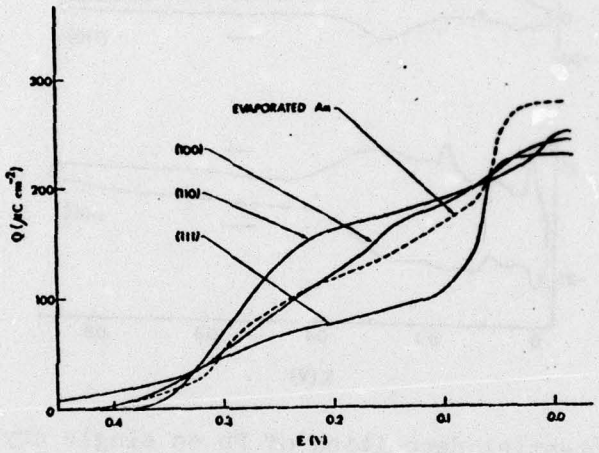

Figure 16. Charge density versus potential curves for the UPD of Pb on single crystal Au, obtained from Fig. 14. [Adzic, Yeager and Cahan (76)].

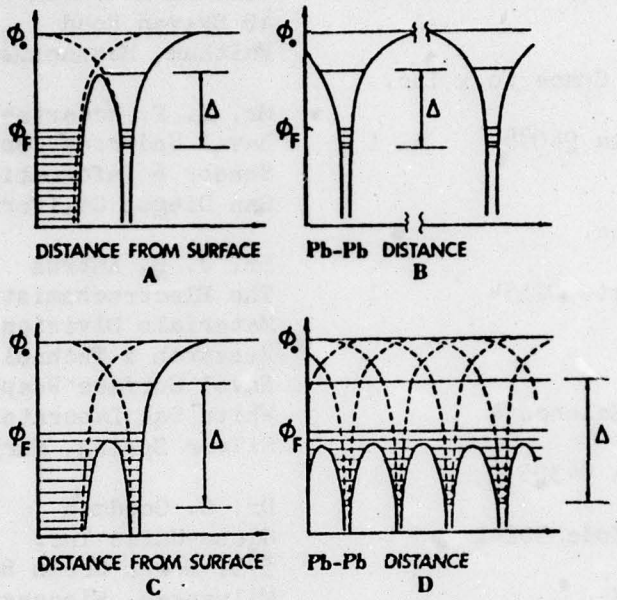

Figure 17. Energy level diagram for lead on gold. A and B, Behavior at low and moderate coverage. C and D, Behavior at high coverage. A and C, Perpendicular to surface. B and D, Parallel to surface. ϕ_∞ Potential energy of electron in unbound state; ϕ_F, Fermi energy; Δ, band width in Pb. Solid curves, combined metal substrate-lead potential curves; dashed lines, parallel curves with no interactions of lead with gold substrate or other adsorbed lead. [Adzic, Yeager, Cahan (76)].

TECHNICAL REPORT DISTRIBUTION LIST

	No. Copies
Dr. M. Eisenberg Electrochimica Corporation 2485 Charleston Road Mountain View, Calif. 94040	1
Dr. Adam Heller Bell Telephone Laboratories Murray Hill, New Jersey	1
Dr. T. Katan Lockheed Missiles & Space Co., Inc. P. O. Box 504 Sunnyvale, California 94088	1
Dr. J. J. Auborn GTE Laboratories, Inc. 40 Sylvan Road Waltham, Massachusetts 02154	1
Dr. R. A. Huggins Stanford University Dept. of Materials Science & Engineering Stanford, California 94305	1
Dr. Joseph Singer, Code 302-1 NASA-Lewis 21000 Brookpark Road Cleveland, Ohio 44135	1
Dr. B. Brummer EIC Incorporated Five Lee Street Cambridge, Massachusetts 02139	1
Library P.R. Mallory & Company, Inc. P. O. Box 706 Indianapolis, Indiana 46206	1
Dr. P. J. Hendra University of Southampton Department of Chemistry Southampton S09 bNH United Kingdom	1
Dr. Sam Perone Purdue University Department of Chemistry West Lafayette, Indiana 47907	1
Dr. Royce W. Murray University of North Carolina Department of Chemistry Chapel Hill, No. Car. 27514	1
Dr. J. Proud GTE Laboratories Inc. Waltham Research Center 40 Sylvan Road Waltham, Massachusetts 02154	1
Mr. J. F. McCartney Naval Undersea Center Sensor & Information Tech. Dept. San Diego, California 92132	1
Dr. J. H. Ambrus The Electrochemistry Branch Materials Division Research & Technology Dept. Naval Surface Weapons Center White Oak Laboratory Silver Spring, Maryland 20910	1
Dr. G. Goodman Globe-Union Inc. 5757 North Green Bay Avenue Milwaukee, Wisconsin 53201	1
Dr. J. Boechler Electrochimica Corporation Attn: Technical Library 2485 Charleston Road Mountain View, Calif. 94040	1
Dr. D. L. Warburton The Electrochemistry Branch Materials Division Research & Technology Dept. Naval Surface Weapons Center White Oak Laboratory Silver Spring, Maryland 20910	1
Dr. R. C. Chudacek McGraw-Edison Company Edison Battery Division P. O. Box 28 Bloomfield, New Jersey 07003	1

TECHNICAL REPORT DISTRIBUTION LIST

	No. Copies
Office of Naval Research Arlington, Virginia 22217 Attn: Code 472	2
Office of Naval Research Arlington, Virginia 22217 Attn: Code 1021P	6
ONR Branch Office 536 S. Clark Street Chicago, Illinois 60605 Attn: Dr. George Sandoz	1
ONR Branch Office 715 Broadway New York, New York 10003 Attn: Scientific Dept.	1
ONR Branch Office 1030 East Green Street Pasadena, California 91106 Attn: Dr. R. J. Marcus	1
ONR Branch Office 760 Market Street, Rm. 447 San Francisco, California 94102 Attn: Dr. P. A. Miller	1
ONR Branch Office 495 Summer Street Boston, Massachusetts 02210 Attn: Dr. L. H. Peebles	1
Director, Naval Research Laboratory Washington, D.C. 20390 Attn: Library, Code 2029 (ONRL) Technical Info. Div. Code 6100, 6170	6 1 1
The Asst. Secretary of the Navy (R&D) Department of the Navy Room 4E736, Pentagon Washington, D.C. 20350	1
Commander, Naval Air Systems Command Department of the Navy Washington, D.C. 20360 Attn: Code 310C (H. Rosenwasser)	1
Defense Documentation Center Building 5, Cameron Station Alexandria, Virginia 22314	12

	No. Copies
U. S. Army Research Office P. O. Box 12211 Research Triangle Park, No. Car. 27709 Attn: CRD-AA-IP	1
Commander Naval Undersea R & D Center SanDiego, California 99132 Attn: Technical Library, Code 133	1
Naval Weapons Center China Lake, California 93555 Attn: Head, Chemistry Division	1
Naval Civil Engineering Laboratory Port Hueneme, California 93041 Attn: Mr. W. S. Haynes	1
Professor O. Heinz Dept. of Physics & Chemistry Naval Postgraduate School Monterey, California 93940	1
Dr. A. L. Slafkosky, Scientific Advisor Commandant of the Marine Corps (Code RD-1) Washington, D. C. 20380	1
Dr. Paul Delahay New York University Department of Chemistry New York, New York 10003	1
Dr. R. A. Osteryoung Colorado State University Department of Chemistry Fort Collins, Colorado 80521	1
Dr. D. N. Bennion University of California Energy Kinetics Department Los Angeles, California 90024	1
Dr. J. W. Kauffman Northwestern University Department of Materials Science Evanston, Illinois 60201	1
Dr. R. A. Marcus University of Illinois Department of Chemistry Urbana, Illinois 61801	1